

This article was downloaded by:

On: 24 January 2011

Access details: *Access Details: Free Access*

Publisher *Taylor & Francis*

Informa Ltd Registered in England and Wales Registered Number: 1072954 Registered office: Mortimer House, 37-41 Mortimer Street, London W1T 3JH, UK



Journal of Macromolecular Science, Part A

Publication details, including instructions for authors and subscription information:

<http://www.informaworld.com/smpp/title~content=t713597274>

Phase Interconnectivity and Environmental Stress Cracking Resistance of Polyethylene: A Crystalline Phase Investigation

Joy J. Cheng^a; Maria A. Polak^b; Alexander Penlidis^a

^a Institute for Polymer Research, Department of Chemical Engineering, University of Waterloo, Waterloo, Ontario, Canada ^b Department of Civil and Environmental Engineering, University of Waterloo, Waterloo, Ontario, Canada

To cite this Article Cheng, Joy J. , Polak, Maria A. and Penlidis, Alexander(2009) 'Phase Interconnectivity and Environmental Stress Cracking Resistance of Polyethylene: A Crystalline Phase Investigation', Journal of Macromolecular Science, Part A, 46: 6, 572 – 583

To link to this Article: DOI: 10.1080/10601320902851801

URL: <http://dx.doi.org/10.1080/10601320902851801>

PLEASE SCROLL DOWN FOR ARTICLE

Full terms and conditions of use: <http://www.informaworld.com/terms-and-conditions-of-access.pdf>

This article may be used for research, teaching and private study purposes. Any substantial or systematic reproduction, re-distribution, re-selling, loan or sub-licensing, systematic supply or distribution in any form to anyone is expressly forbidden.

The publisher does not give any warranty express or implied or make any representation that the contents will be complete or accurate or up to date. The accuracy of any instructions, formulae and drug doses should be independently verified with primary sources. The publisher shall not be liable for any loss, actions, claims, proceedings, demand or costs or damages whatsoever or howsoever caused arising directly or indirectly in connection with or arising out of the use of this material.

Phase Interconnectivity and Environmental Stress Cracking Resistance of Polyethylene: A Crystalline Phase Investigation

JOY J. CHENG¹, MARIA A. POLAK² and ALEXANDER PENLIDIS^{1,*}

¹*Institute for Polymer Research, Department of Chemical Engineering, University of Waterloo, Waterloo, Ontario, N2L 3G1, Canada*

²*Department of Civil and Environmental Engineering, University of Waterloo, Waterloo, Ontario, N2L 3G1, Canada*

Received and Accepted January 2009

Studies of the effect of inter-lamellar linkages on environmental stress cracking resistance (ESCR) of polyethylene have traditionally focused on changes in the amorphous phase. Since polyethylene is a semi-crystalline polymer, the crystalline phase also plays an important role in the mechanical behavior of the polymer. In this work, percentage crystallinity and lamella thickness of several high density polyethylene (HDPE) resins were studied to determine their effect on ESCR. It was observed that when average molecular weights of resins were widely different, these crystalline phase indicators could not adequately reflect changes in interconnectivity between crystalline and amorphous phases of polyethylene, and therefore, could not be correlated to ESCR of the resins in a straightforward fashion. Since polyethylene lamellae are three-dimensional crystals, the study of the crystalline phase effect on ESCR was extended to investigating the lateral surface characteristics of the lamella. An increase in ESCR was observed with increases in lateral lamella area of resins. It was postulated that a larger lateral lamella area results in higher probability of formation of inter-lamellar linkages. This increase in phase interconnectivity directly results in increasing ESCR of resins.

Keywords: Crystalline phase, environmental stress cracking resistance, inter-lamellar links, phase interconnectivity, polyethylene

1 Introduction

Polyethylene (PE) is one of the most versatile commercial polymers today. The semi-crystalline nature of PE allows it to operate over a wide range of temperatures. The crystalline phase of the polymer gives it strength, while the amorphous phase allows PE to be flexible. High density polyethylene (HDPE) is used in the manufacturing of a variety of products, from paint containers to gas line pipes. Compared to pipes of other materials, HDPE pipes have the advantages of being light-weight, corrosion-resistant and easy to install. However, one of the major problems for polyethylene in pipe and other structural applications is environmental stress cracking (ESC). HDPE pipes that should have a service life of fifty years can fail in just one year due to ESC (1). Therefore, environmental stress cracking resistance (ESCR) of polyethylene is of key interest to manufacturers and researchers alike.

The semi-crystalline nature of PE influences many of its mechanical properties (2). Melt-crystallized polyethylene

has a spherulite morphology, where lamellae made up of spherulites are embedded in a matrix of amorphous material (3, 4). The structure of lamellae generally consists of regular chain-folding arrangements with the molecular chains perpendicularly aligned to the lateral lamellar surfaces. The regular chain-folding growth of a lamella results in crystals with lateral direction dimensions (1–50 μm) being much larger than their thickness (2–25 nm) (5, 6).

The bulk crystallinity of polyethylene is largely influenced by the processing conditions. Slow cooled and annealed materials have higher crystallinity than quenched polyethylene (7–10). Under the same processing conditions, the crystallinity of PE is influenced by molecular weight and chain structure. The crystallinity of PE increases with increasing molecular weight (8) because longer polymer chains can form larger lamellae. The presence of short chain branching (SCB) hinders the lamella formation process, because chains with SCB cannot be readily incorporated into the lamellar structure. Thus, smaller lamellae are formed and the crystallinity of PE is decreased (11, 12). Research has shown that side branches longer than two-carbon atoms cannot be incorporated into the lamella (11). Linear low density polyethylene (LLDPE) with its many side chain groups is known to have lower crystallinity than high density polyethylene, which has fewer side chains (9).

*Address correspondence to: Alexander Penlidis, Institute for Polymer Research, Department of Chemical Engineering, University of Waterloo, Waterloo, Ontario, N2L 3G1, Canada. E-mail: penlidis@cape.uwaterloo.ca

Environmental stress cracking is a form of brittle fracture (13). The mechanism of failure is believed to be a process of disentanglement of inter-lamellar linkages/connections (tie-molecules (13) and entanglements (14)) from the crystalline phase. Research has shown that ESCR of HDPE increases with increasing molecular weight (MW) and SCB content. High MW indicates the presence of long polymer chains that can crystallize into two or more lamellae and form inter-lamellar connections that improve ESCR (10, 15, 16). High SCB content disrupts the formation of the crystalline phase and forces polymer chains into the amorphous phase. Increase in amorphous phase material is believed to lead to formation of more tie-molecules (17, 18). SCB also hinders chain slippage from a lamella by acting as an "anchor point" (19). Since inter-lamellar linkages are an important factor influencing ESCR of polyethylene, most research on ESCR in the past has traditionally focused on the amorphous phase of the material.

Published work on the effect of the crystalline phase of PE on ESCR has revealed unclear relationships. Earlier work by Hittmair and Ullman (20) showed an increase in ESCR with increase in crystallinity. A probabilistic approach to the calculation of tie-molecule concentration, as developed by Huang and Brown (15, 21), stated that ESCR of polyethylene is inversely proportional to the thickness of the lamella, because more chains of lower MW can act as tie-molecules when the lamellae are thinner. This implies an increase in ESCR with decreasing crystallinity. Lu et al. (7) observed that annealing of PE below 113°C improves its slow crack growth resistance (SCGR). At annealing temperatures above 113°C, the SCGR of PE decreases with increasing anneal temperature. Lu et al. (7) attributed the former observation to an increase in crystal perfection with annealing. The latter observation was concluded to be caused by a decrease in tie-molecules due to increased incorporation of chains into the crystalline phase. Most experimental observations of the relationship between PE crystallinity and ESCR were made as a side note on research about the effect that molecular characteristics have on tie-molecule concentration (19, 22, 23). These publications generally show that a decrease in crystallinity is merely a side effect of an increase in inter-lamellar links due to an increasing SCB content.

There is no doubt that the influence of crystallinity on ESCR of polyethylene is complicated and further clarification is needed. Previous work on crystallinity and ESCR was mostly restricted to a few resins of limited MW and molecular weight distribution (MWD) range. In the work presented herein, high density polyethylene resins of a wide range of MW and MWD are studied to investigate and quantify the effect of crystalline phase on ESCR. ESCR of resins is associated to classical crystalline phase property indicators, such as crystallinity and lamella thickness. In addition to these indicators, a lamella lateral surface analysis and its effect on ESCR is pursued further.

2 Experimental

2.1 Size Exclusion Chromatography - SEC

Molecular weight (MW) and molecular weight distribution (MWD) of resins were characterized using high temperature size-exclusion (gel permeation) chromatography (SEC/GPC). The equipment used was a Waters GPCV 150+ equipped with a refractive index detector and a Viscotek 150R viscometer (operating at 140°C, using 1,2,4-trichlorobenzene (TCB) as solvent). Average molecular weights were calculated based on narrow polystyrene standards.

2.2 ¹³C-NMR

Short chain branch (SCB) content per one thousand carbon atoms of resins was determined using Carbon-13 nuclear magnetic resonance spectroscopy (¹³C-NMR).

¹³C-NMR analysis was done with an AVANCE 500 Bruker NMR. Experiments were run at 120°C. Each sample consisted of 5 mg of polymer dissolved in trichlorobenzene, with trichloroethylene (TCE) as the tracer.

2.3 Differential Scanning Calorimetry (DSC)

Differential scanning calorimetry was used to determine the crystallinity of polyethylene resins. The analysis was carried out on a TA Instruments DSC 2920 module. A 10°C/min ramp from 40°C to 240°C was used for all samples. The theoretical value of heat of fusion for a 100% crystalline polyethylene used in the calculation of percent crystallinity of samples was 293.6 J/g (24). The sample size used per run was approximately 5 mg.

The peak melting temperature from DSC was used for the calculation of the lamella thickness based on the well established Gibbs-Thomson equation (Equation 1) (25).

$$T_m = T_m^o \left(1 - \frac{2\sigma_e}{\Delta h_m l} \right) \quad (1)$$

T_m is the observed melting temperature of the resin at the peak of the DSC curve. l is the lamella thickness. The other parameter values used for polyethylene were based on the work by Wlochowicz and Eder (25). $T_m^o = 415$ (K) is the equilibrium melting temperature of an infinite crystal; $\sigma_e = 60.9 \times 10^{-3}$ (Jm⁻²) is the surface free energy of the basal plane; and $\Delta h_m = 2.88 \times 10^8$ (Jm⁻³) is the enthalpy of fusion per unit volume.

2.4 X-Ray Diffraction

2.4.1. Wide angle X-ray scattering (WAXS)

Two types of X-ray scattering techniques were used in this study. The first was the standard X-ray diffraction, also known as wide angle X-ray scattering (WAXS). Discs of 25mm diameter and 1mm thickness were

compression-molded at 190°C, 10000 lbf and then quench cooled. WAXS experiments were conducted using a Stoe two circle goniometer in a Bragg-Brentano geometry equipped with a Moxtek solid state detector and sourced by an Enraf Nonius 571 rotating anode generator. The scattering angle was from 6° and greater. Scattering intensity maxima were observed at 21.5° and 23.9°. The integrated area of the scattering intensity peaks has been shown to be proportional to the mass of the crystalline phase (26). Therefore, the overall crystallinity of a semi-crystalline polymer can be calculated using Equation 2.

$$\%crystallinity = \frac{\int_0^\infty I_{cr}}{\int_0^\infty I_{cr} + \int_0^\infty I_{am}} \times 100 \quad (2)$$

I_{cr} is the scattering intensity of the crystalline phase peaks. I_{am} is the scattering intensity of the amorphous phase, taken as the remainder area under the total scattering curve that is outside of the crystalline peaks.

2.4.2. Small-angle X-ray scattering (SAXS)

Small-angle X-ray scattering tests were used to obtain long period (L) measurements of resins. Experiments were carried out on a Bruker AXS NaoStarU with a Hi-Star 2D detector. Compression-molded discs of 25 mm diameter and 1 mm thickness were used, as in the WAXS experiments. The long period (L) of each resin was calculated based on Equation 3, with λ fixed from the equipment, and ε and n obtained from the spectra. Lamella thickness of polyethylene was subsequently calculated using Equation 4 and the long period (L) information, combined with the results of percentage crystallinity information either from the DSC or the WAXS methods.

$$L\varepsilon = n\lambda \quad (3)$$

L -long period, ε - Bragg's angle of the intensity maximum, n -level of scattering (usually has the value of 1), λ - wavelength of the X-ray

$$Lamella\ thickness = \%crystallinity \times L \quad (4)$$

2.5 Environmental Stress Cracking Resistance (ESCR)

Environmental stress cracking resistance of polyethylene was measured using the notch constant load test (NCLT). Experiments were run following the guidelines of ASTM D5397, at 50°C in a temperature bath containing 10% Igepal (nonyl phenyl ether glycol, $C_{19}H_{19}-C_6H_4-O-(CH_2CH_2O)_8-CH_2CH_2OH$) solution. A load at 15% of the yield stress of the material was used to ensure fracture occurred in the brittle failure region (1). Dogbone shaped samples were cut out from plates of polymer made by compression molding at 190°C \pm 5°. Specimen dimensions are shown in Figure 1. The thickness of the sample was 1.8 \pm

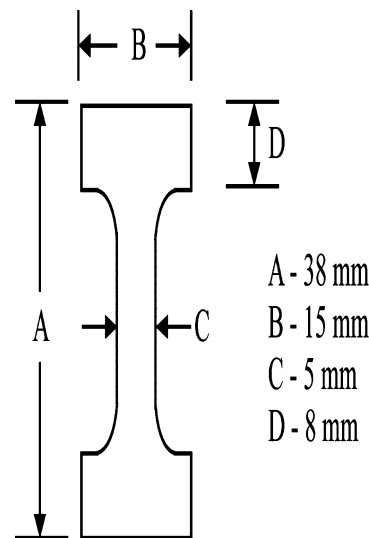


Fig. 1. Dogbone dimensions for NCLT.

0.1 mm. A notch was introduced into the samples at the middle of the dogbone using a sharp razor blade. For our tests, we used a notch that was 40% of the thickness of the sample instead of 20% as indicated by ASTM D5397. Conclusions on ESCR results were not affected by this modification. A detailed discussion regarding the effects of notch depth on NCLT results can be found in Cheng et al. (27).

3 Results and Discussion

3.1 Environmental Stress Cracking Resistance

High density polyethylene (HDPE) resins from various industrial sources have been considered in this project. These resins (Table 1) have been designed for a variety of applications. PE1-3 are blow molding resins, PE4-5 are injection molding resins, and PE7-10 are pipe resins. Different resin characteristics are listed in Table 1. M_n , M_w , and M_z stand for number-average, weight-average and z-average molecular weights, respectively. PDI is the polydispersity index based on M_w/M_n . The SCB column gives the number of short chain branches per one thousand carbon atoms for the resins. All resins were copolymers with the butyl group as a side chain. PE9 also had a small amount of methyl group side chains.

The ESCR values of the pipe resins were found to be much higher than all the other resins (Table 1). Since pipe resins are designed to have high ESCR (28), this is expected. PE7, PE9 and PE10 are PE100-grade pipe resins. PE8 is a PE80-grade pipe resin, and so it is expected to have lower ESCR than a PE100-grade. The ESCR values in Table 1 reflect the difference in pipe resin grading. Of all the PE100 resins, PE10 has the “best” (largest) ESCR. Samples of PE10 did not fail in NCLT even after 3000 hours. This is

Table 1. Material characteristics of resins

Resin	ESCR (hours)	M_n (kg/mol)	M_w (kg/mol)	M_z (kg/mol)	PDI	SCB (/1000C)
PE1	4.8	16.3	127.5	814.0	7.8	2.8
PE2	1.2	15.7	118.5	837.1	7.6	1.1
PE3	2.8	17.9	140.1	889.8	7.8	0.9
PE4	3.6	19.7	79.4	239.3	4.0	3.8
PE5	N/A	11.4	49.7	157.8	4.4	7.0
PE6	N/A	14.0	62	195.0	4.4	4.7
PE7	1396	11.8	222.8	1593.5	18.9	4.3
PE8	198	14.0	202.1	1398.4	14.4	4.5
PE9	843	10.4	217.9	1244.2	20.9	7.0
PE10	>3000	5.9	315.4	2129.3	53.3	11.8

due to the higher MW of PE10. For non-pipe resins, PE1 and PE4 have the best ESCR values. Two resins, PE5 and PE6, could not be tested using NCLT because they were brittle and could not survive the notching process.

A higher ESCR value is associated with higher MW because longer chains can form inter-lamellar links more effectively (15). PE7-10 have higher MW than PE1-4. Hence, they exhibited higher ESCR (Table 1). The influence of the higher MW tail of the MWD is reflected more so in the M_z -average molecular weight values than in the other averages. In general, resins with higher M_z values have higher ESCR. Another indicator that can reflect presence of large chains in a polymer system is the PDI. PE7-10 have larger PDI values than PE1-4. A large PDI value indicates a MWD with a large high-MW-end-tail, hence, the presence of more chains of higher MW in the system. Higher MW chains improve the ESCR of the resin, thus resins with high PDI (Table 1) have higher ESCR.

Differences in MW alone cannot explain differences in ESCR values. Comparing PE1-4, PE3 has the highest MW of the four resins, yet its ESCR is relatively low. Looking at the SCB/1000C atoms measurement of these resins, it

can be seen that PE2 and PE3 have lower SCB content than the others. The lower SCB content gives these resins lower ESCR. As mentioned earlier, an increase in SCB content is known to increase formation of inter-lamellar links and prevent chain slippage from lamellae, hence, it overall improves the ESCR of polyethylene.

3.2 Crystallinity and Lamella Thickness

Crystalline phase characteristics of resins were investigated using DSC and X-ray diffraction methods. Since percentage crystallinity and lamella thickness values were obtained using both techniques, in order to avoid confusion a definition of certain terms is in order from the outset of this section. In the following, DSC-crystallinity refers to the percentage crystallinity of polymer obtained using the DSC method outlined in section 2.3; WAXS-crystallinity is the percentage resin crystallinity based on Equation 2 in section 2.4. DSC-lamella thickness is calculated using Equation 1 and the peak melting temperature from the DSC curve. On the other hand, SAXS-lamella thickness refers to lamella thickness based on the long period information from SAXS (Equations 3 and 4 of section 2.4).

3.2.1. Resin crystallinity measurements

Information regarding percentage crystallinity of resins is presented in Table 2. All resins have crystallinity values that are 50% or higher, characteristic of HDPE. Crystallinity values of resins in this study mainly reflect the SCB influence. Presence of SCB is known to interrupt formation of crystalline lamellae; hence, higher SCB content decreases the overall crystallinity of a polymer (11). PE10 has lower crystallinity than other resins because of higher SCB content (Table 1). In contrast, PE2 and PE3 have higher crystallinity than all other resins because of their low SCB content.

From Table 2, it is observed that the WAXS-crystallinity values are systematically higher than the DSC-crystallinity

Table 2. Crystallinity and lamella thickness of resins

	DSC		SAXS			
	DSC %crystallinity	WAXS %crystallinity	Melt temperature (°C)	Lamella thickness (nm)	L - long period (nm)	Lamella thickness (nm)
PE1	55.4%	61.9%	130.5	15.3	24.27	13.3
PE2	58.8%	70.2%	135.5	26.8	28.68	16.7
PE3	57.9%	66.4%	134.1	22.3	25.53	14.7
PE4	55.1%	60.2%	130.1	14.7	23.31	12.7
PE5	53.9%	61.1%	129.1	13.6	19.94	10.7
PE6	56.6%	63.0%	129.8	14.4	21.60	12.1
PE7	53.3%	60.0%	130.7	15.5	24.75	13.1
PE8	56.2%	60.3%	128.6	13.1	26.61	14.8
PE9	61.5%	63.3%	129.9	14.6	24.27	14.9
PE10	51.1%	59.5%	127.0	11.7	24.54	12.4

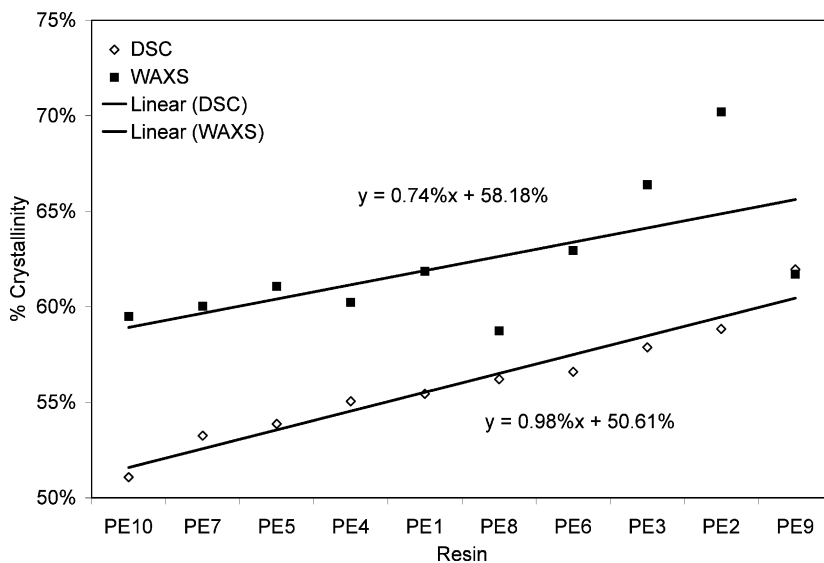


Fig. 2. Percentage crystallinity of resins by DSC and WAXS.

values. Other published work also observed that the WAXS method tended to give a higher measured crystallinity value than that from the DSC method (29, 30). The differences between crystallinity determinations obtained using the two methods are believed to be due to the different nature of the two methods. DSC-crystallinity is based on the enthalpy of fusion of polymer crystals, whereas WAXS-crystallinity is based on scattering intensity peaks. Thus, the two methods reflect aspects of the crystalline phase that are fundamentally different from each other. Therefore, differences between the DSC-crystallinity and WAXS-crystallinity values can be expected. In Figure 2, the crystallinity values of resins are plotted in ascending order. The linear regression confirmed (as expected) that the DSC-crystallinity and WAXS-crystallinity have similar slope values, but different intercepts. The WAXS-crystallinity has a larger intercept value (58.18%) than the DSC-crystallinity (50.61%). This result indicates that despite the differences in actual crystallinity values between the two methods, the trend in resin crystallinity is the same from both methods. This consistent trend (Figure 2) confirms the real crystallinity differences between the resins.

Independently replicated tests and repeats were carried out on both DSC and WAXS determinations in order to investigate further the precision of the measurements. For DSC, the average coefficient of variation (standard deviation/mean) for the measurements was 0.059, based on an average of 10 independently replicated measurements per resin, thus demonstrating the good reproducibility of the DSC measurements. For WAXS experiments, being not such a commonly used or studied technique, independent replication with selective resins started with step one, namely the molding of plates. ANOVA (ANalysis Of VAriance) technique was used to investigate different sources of variability. In Table 3, ANOVA of PE9 is presented. The

F-observed value is smaller than the F-critical value of 7.71 according to a 5% significance level and (1,4) degrees of freedom. This means that the test procedure does not contribute statistically significant variability to the measurements. Therefore, the WAXS measurements can be trusted to reflect material property differences.

3.2.2. Lamella thickness measurements

Lamella thickness (DSC and SAXS) information of resins is also presented in Table 2. The values of lamella thickness are within the range of reported lamella thickness values for polyethylene (6). The differences in lamella thickness values seem to follow the differences in SCB content of resins. Resins with lower SCB content (PE2 and PE3) have thicker lamellae.

Overall, the lamella thickness values obtained from DSC and SAXS are similar. This can be seen in Figure 3, where the ratio of the DSC-lamella thickness value to the SAXS-lamella thickness value fluctuates about 1. However, for PE2 and PE3 the DSC method gives a much higher lamella thickness value than the SAXS method (Table 2). SAXS long period is a measurement of the average periodic spacing in a polymer system (26). Therefore, SAXS-lamella thickness is a measurement of the average lamella thickness of the system. On the other hand, the DSC result is based on the peak melting temperature, which is associated with the most abundant lamella thickness present in a

Table 3. ANOVA of WAXS measurements for PE9

	<i>df</i>	<i>SS</i>	<i>MS</i>	<i>F</i>
Different molding of plates	1	0.00144	0.00144	6.26
Same molding of plates	4	0.00094	0.00023	
Total	5	0.00238		

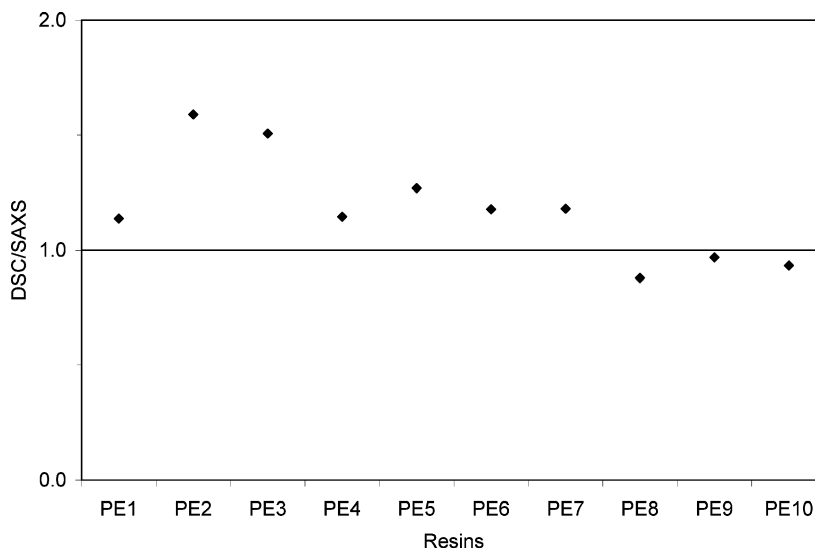


Fig. 3. Ratio of DSC-lamella thickness value to SAXS-lamella thickness value.

polymer system. The SAXS-lamella thickness is analogous to the mean of a data set, while the DSC-lamella thickness is the mode of the data set. Therefore, some difference between the most abundant lamella thickness value and the average lamella thickness value can be understood.

SAXS-lamella thickness values are calculated using the SAXS long period information and the percentage crystallinity of the resin (Equation 4). In this study, resin crystallinity was obtained from both the DSC and WAXS methods. SAXS-lamella thickness values presented in Table 2 are calculated using DSC-crystallinity. It was established in section 3.2.1 that the DSC-crystallinity and the WAXS-crystallinity showed the same trends. Therefore, regardless of which crystallinity measurement is used, the calculated SAXS-lamella thickness would show the same trend. This

fact is confirmed by Figure 4, where the ratio of SAXS-lamella thickness calculated based on DSC-crystallinity and WAXS-crystallinity is plotted. The ratio is about 1, thus indicating that lamella thickness values are in good agreement regardless of which crystallinity determination alternative is used. Henceforth, in the remainder of the paper, discussions regarding SAXS-lamella thickness values are based on DSC-crystallinity.

Lamella thickness values for PE are reported in nanometres. Therefore, the precision of these determinations is important. For DSC peak melting temperature, the average coefficient of variation is 0.009, based on an average of 10 independent replicate measurements per resin. Therefore, once again, the precision of SAXS experiments was explored using selective independently replicated tests and

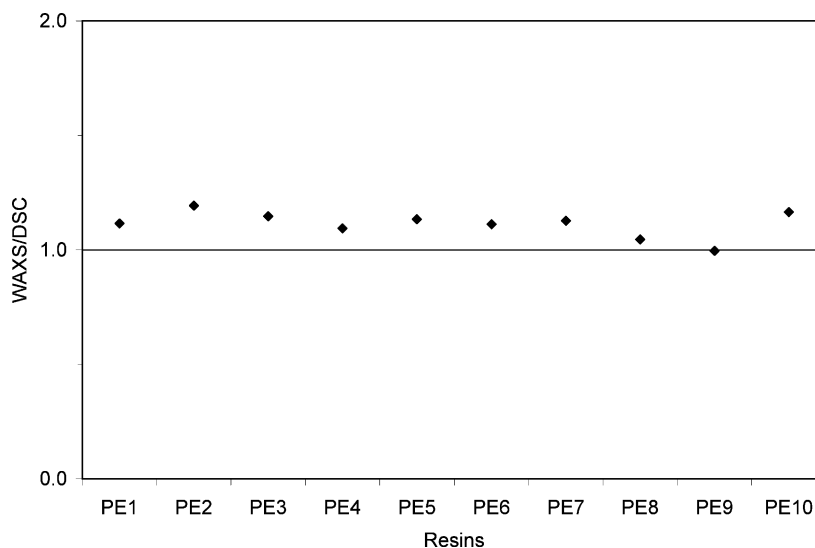


Fig. 4. Ratio of lamella thickness calculated using WAXS-crystallinity and DSC-crystallinity.

Table 4. ANOVA of SAXS measurements for PE9

	<i>df</i>	<i>SS</i>	<i>MS</i>	<i>F</i>
Same molding of plates	4	0.22803	0.05700	8.333
Different molding of plates	1	0.00684	0.00684	
Total	5	0.23487		

ANOVA. Independent replication started again from the sample molding step. For comparative purposes, the analysis results for PE9 are presented (Table 4). The *F*-observed value in Table 4 is smaller than the *F*-critical value of 224.6 (based on a 5% significance level and (4,1) degrees of freedom), indicating again that there is no significant contribution to the measurement variability by the test procedure.

3.3 Crystalline Phase Characteristics and ESCR

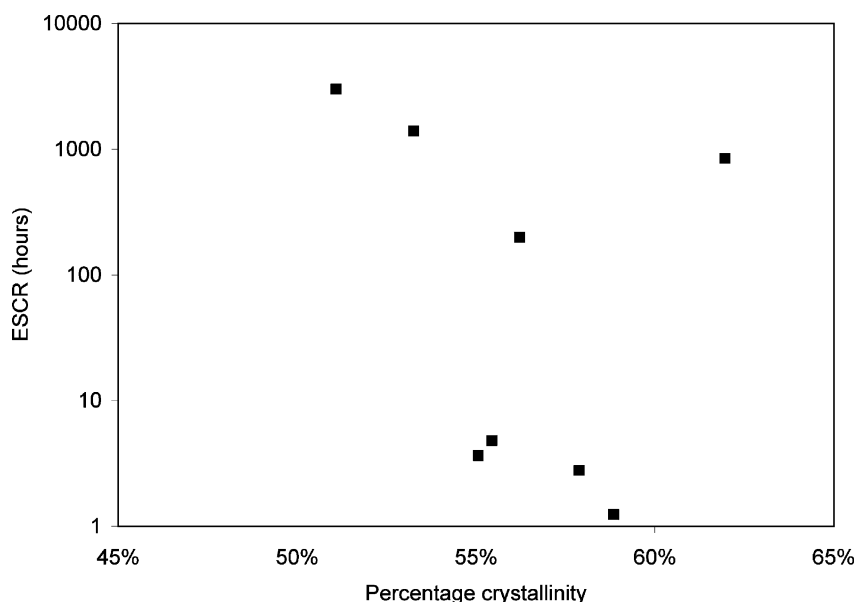
3.3.1. Crystallinity and ESCR

The coexistence of crystalline and amorphous phases gives rise to the semi-crystalline nature of polyethylene. Mechanical behavior of PE is influenced by both phases. ESCR of polyethylene is believed to be mainly controlled by the amorphous phase of the material. PE resins with more inter-lamellar linkages have higher ESCR. However, the number of inter-lamellar links in the amorphous phase does not matter if their ends could not be fixed in the crystalline phase. This is a relationship of “anchors” and “ropes”. The precise number of inter-lamellar connections in the amorphous phase cannot be directly measured despite a variety of approaches that have been attempted (6, 31). Since the number of “ropes” cannot be measured, we decided to look at the nature of the “anchor”.

It is well established that an increase in crystallinity increases the tensile yield strength of polyethylene (9). Weight percentage crystallinity is the most often quoted crystalline phase measurement for polyethylene. In Figure 5, ESCR is plotted against the DSC-crystallinity for all resins in this study. Log scale is used because of the large differences in ESCR values of the resins (Table 1). The data points are rather scattered in Figure 5, indicating that no clear correlation exists between percentage crystallinity and ESCR. The lack of an established correlation pattern is most likely due to major MW differences between resins (Table 1). PE crystallinity is strongly influenced by SCB content. On the other hand, ESCR of polyethylene is influenced first by MW, and only secondarily influenced by SCB content. This lack of correlation pattern when the MW range is wide may explain the inconsistent observations reported regarding crystallinity and ESCR in the literature.

On closer inspection of the lower MW resins (PE1-4 in Table 1), there exists a trend of lower crystallinity (both DSC-crystallinity and WAXS-crystallinity) associated with higher ESCR (Table 2). PE1 and PE4 have lower crystallinity compared to PE2 and PE3 because of higher SCB content (Table 1). SCB is known to disrupt lamella formation and decrease crystallinity (11). Lower crystallinity means there is a higher percentage of amorphous phase, and this higher percentage of amorphous material could lead in its turn to formation of more inter-lamellar linkages, which is known to increase ESCR (15).

For the high MW range HDPE resins in this study (PE7-10), the relationship between crystallinity and ESCR is more complicated. PE9 has one of the highest crystallinity values of all resins, yet its ESCR is high (see Tables 1 and 2). It seems that when MW is high, an increase in crystallinity does not result in large reduction of chains in the

**Fig. 5.** ESCR vs. DSC-crystallinity for PE1-4 and PE7-10.

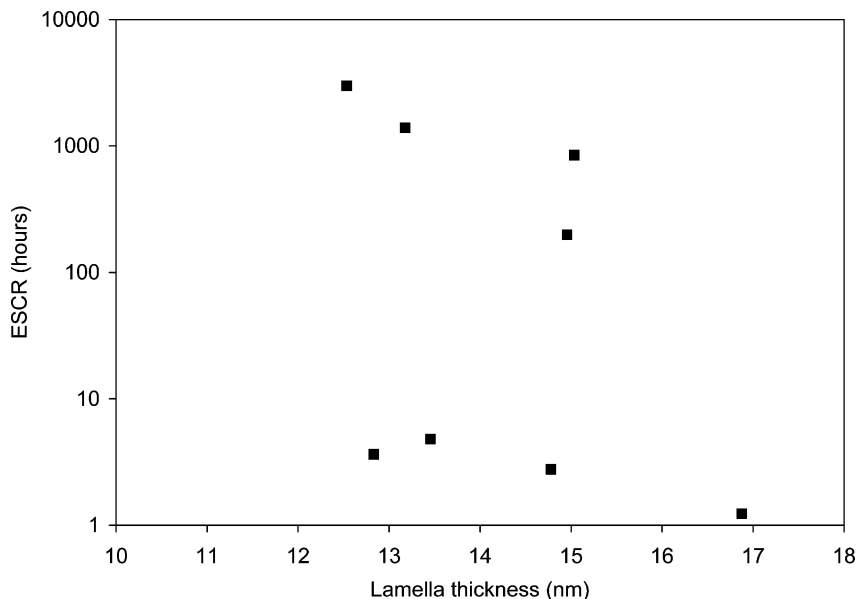


Fig. 6. ESCR vs. SAXS-lamella thickness for PE1-4 and PE7-10.

amorphous phase because the chains are of sufficient length to form crystalline lamellae and amorphous links. When there is a sufficient number of inter-lamellar links, large crystals may in fact improve ESCR of the material because the crystals are stronger. This confirms observations by Lu et al. (7) on the annealing effect on slow crack growth of PE. It needs to be noted that this postulation only applies to polyethylene copolymers, because high MW high crystallinity PE homopolymer is known to have poor/lower ESCR (32).

3.3.2. Lamella thickness and ESCR

Lamella thickness is another frequently used crystalline phase indicator for polyethylene. For resins in this study, DSC-lamella thickness and SAXS-lamella thickness values

were presented in Table 2. Lamella thickness has been proposed to be inversely related to formation of tie-molecules (15), therefore, inversely related to ESCR of PE. For resins of similar MW (PE1-3), smaller lamella thickness values can be seen to correlate with higher ESCR values (Tables 1 and 2). PE1 has thinner lamellae and higher ESCR than PE2-3 because of its higher SCB content than the other two resins. However, when the same analysis is extended to all resins in this study, no significant correlation can be observed between lamella thickness and ESCR of resins. In Figure 6, a plot of ESCR and SAXS-lamella thickness is presented. SAXS-lamella thickness values are used because they represent average lamella thickness as discussed in section 3.2.2. The lack of trend for the data points in Figure 6 indicates that when MW differences of materials

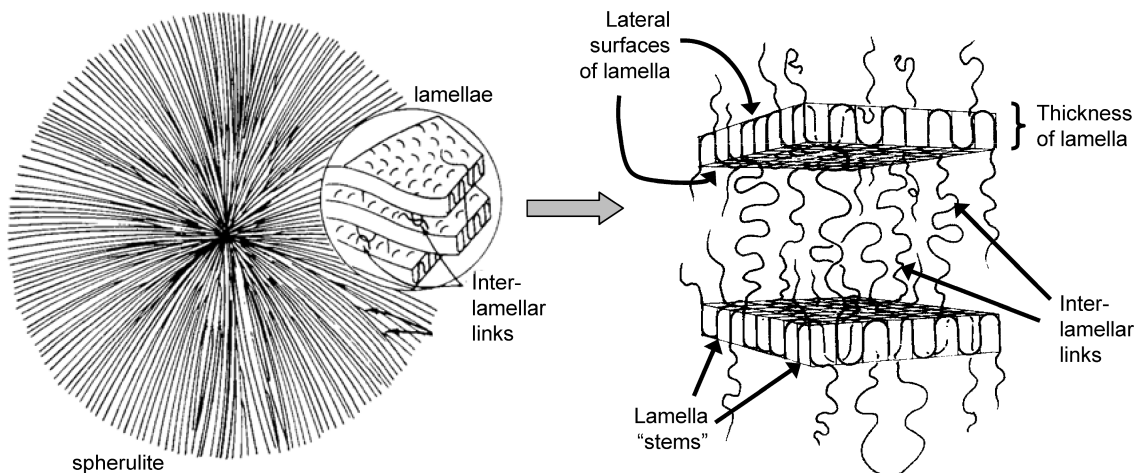


Fig. 7. Schematic illustration of spherulite and lamella, adapted from ref. (13, 35).

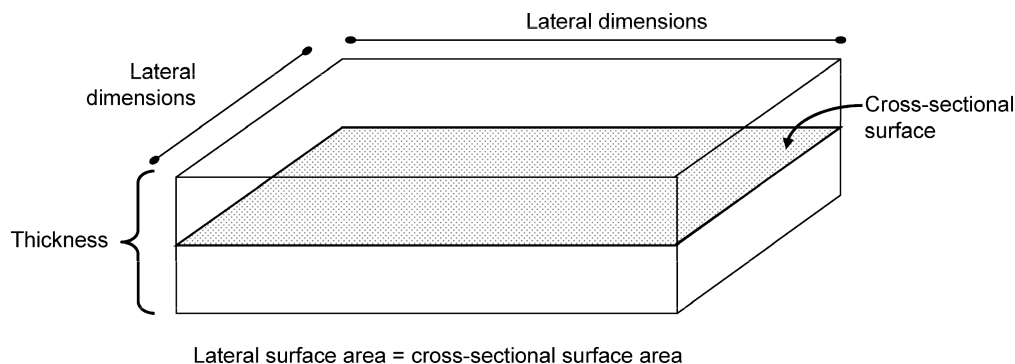


Fig. 8. Rectangular prism representation of lamella.

are large, there is no easily established correlation between lamella thickness and ESCR of polyethylene.

3.3.3. Lamellar lateral surface and ESCR

A tough polymer has superior brittle crack resistance. It was recently proposed that the toughness of semi-crystalline polyester films depends on the interconnectivity of their crystalline and amorphous phases (33). It seems that changes in phase interconnectivity could not be adequately reflected in changes in crystallinity and lamella thickness of resins. Inter-lamellar links reside predominantly at the lateral lamella surface (34), as illustrated in Figure 7, therefore changes in lamella lateral surface area should reflect changes in phase interconnectivity.

The crystalline phase of polyethylene consists of spherulites made up of flat shape lamellae (Figure 7), where the lateral dimensions of the crystals are much larger than their thickness. Researches have shown that inter-lamellar links form part of the lamella “stems” and protrude from the crystal surfaces more or less perpendicular to the lateral dimensions (6). It has also been reported that 10% or more of lamella “stems” consist of inter-lamellar connections (6, 36). Therefore, it is reasonable to presume that PE with larger lamella lateral surface areas will have more inter-lamellar linkages and higher phase interconnectivity.

Unlike a solid catalyst, the surface area of polyethylene lamellae cannot be measured using a technique such as BET surface analysis. However, the total lateral surface area of lamellae can be calculated based on some understanding of polyethylene microstructure. Since its lateral dimensions are much larger than its thickness, a lamella can be viewed as a thin flat crystal. PE lamellae are often represented by rectangular blocks in micromechanical simulations for mechanical response studies (37). In this study lamellae are also viewed as thin rectangular prisms (Figure 8.). For a prism of known volume, its cross-sectional area can be calculated based on its height. The same idea can be applied to rectangular lamella crystals as well. Then the total lamella lateral surface area would be equal to twice that of its cross-sectional area because a lamella has two lateral surfaces. However, inter-lamellar links extended from the

lower lateral surface of one crystal are associated with links anchored in the upper lateral surface of the lamella below (see Figure 7). Therefore, when calculating lamella lateral surface area in relation to phase interconnectivity, only one side of the lamella should be accounted for. The lamella lateral surface area per mole, henceforth referred to simply as lamella area, can be calculated from the following equation:

$$\begin{aligned} \text{lamella area [m}^2/\text{mole]} \\ &= \frac{\text{specific volume of crystal [m}^3/\text{kg]} \\ &\quad \bullet \text{MW of crystal [kg/mole]} \end{aligned} \quad (5)$$

The packing of chains in the crystalline lamella is governed by the steric interaction of molecules (6). Therefore, PE crystals can be considered to be incompressible and of constant density. The lamella density is very nearly equal to the unit-cell density of a perfect polyethylene crystal, which is equal to 1 kg/m³ (24). Therefore, the specific volume of a PE crystal is 1 m³/kg.

The lamella thickness value can be obtained from either DSC or SAXS measurements (Table 2). To simplify calculations, it is assumed that there is no variation of thickness within each lamella crystal, and hence lamella thickness

Table 5. Lamella area estimates of resins

	Lamella area based on DSC-lamella thickness (m ² /mole)	Lamella area based on SAXS-lamella thickness (m ² /mole)
PE1	4.62E+09	5.25E+09
PE2	2.60E+09	4.13E+09
PE3	3.64E+09	5.49E+09
PE4	2.97E+09	3.41E+09
PE5	1.96E+09	2.49E+09
PE6	2.44E+09	2.87E+09
PE7	7.63E+09	9.00E+09
PE8	8.64E+09	7.59E+09
PE9	9.27E+09	8.98E+09
PE10	1.38E+10	1.29E+10

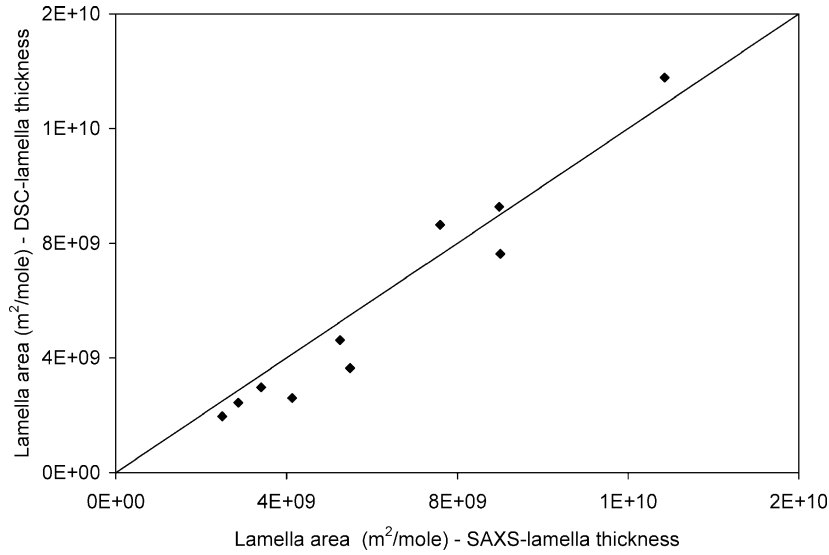


Fig. 9. Lamella area estimates based on SAXS-lamella thickness and DSC-lamella thickness measurements.

values can be applied to the entire crystal. As with other properties of a polymer, such as MW, there is a distribution of lamella thickness in a polymer system. In our calculations the lamella thickness distribution is assumed to be uniform because the average lamella thickness value (SAXS-lamella thickness) and most abundant lamella thickness value (DSC-lamella thickness) for resins were shown to be similar (see section 3.2.2).

The MW of a crystal for a resin is taken as its M_w (Table 1) multiplied by its percentage crystallinity (Table 2). The DSC-crystallinity and WAXS-crystallinity values have been shown to exhibit the same trends in section

3.2.1. Separate crystal-MW calculations based on these two crystallinity measurements would only be different by a scaling factor, therefore, only DSC-crystallinity values were used in subsequent calculations.

The lamella area calculated based on Equation 5 is an aggregate representation of the total lamella lateral surface area in a polymer system. In Table 5, lamella thickness values are shown based on calculations done using SAXS-lamella thickness values and DSC-lamella thickness values. As mentioned in section 3.2.2, SAXS-lamella thickness is a measure of the average lamella thickness, while DSC-lamella thickness values represent the most abundant

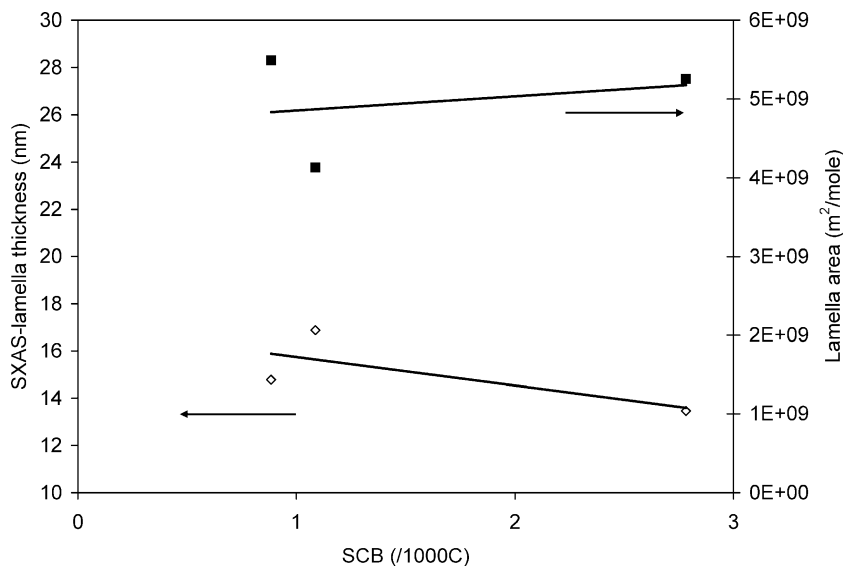


Fig. 10. SCB influence on lamella thickness and lamella area for PE1-3.

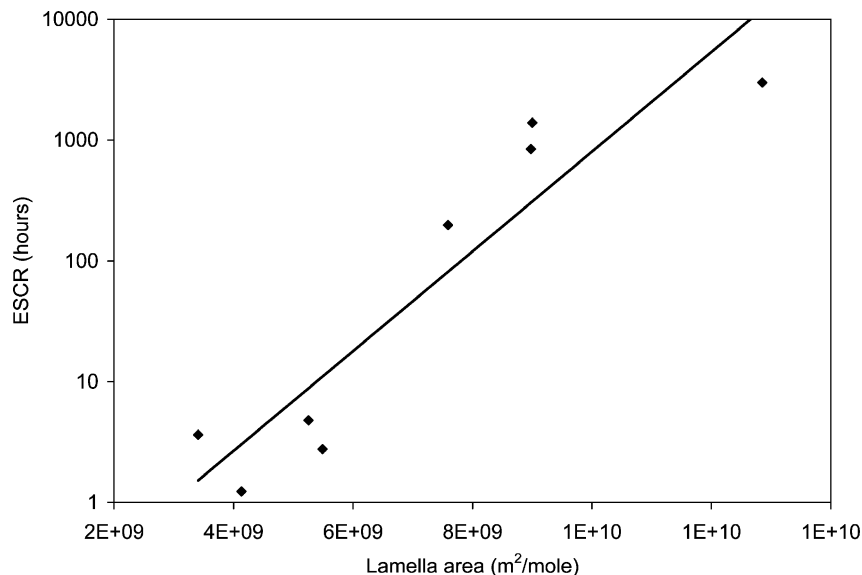


Fig. 11. ESCR vs. lamella area of resins based on SAXS-lamella thickness values.

lamella thickness. The pipe resins (PE7-10) have larger lamella area values than non-pipe resins (PE1-6). PE10 has the largest lamella area value of all resins. In Figure 9, the lamella area values calculated based on SAXS-lamella thickness and DSC-lamella thickness are plotted against each other. It can be seen that lamella area values based on DSC and SAXS methods align at the $y = x$ line, indicating that both type of thickness measurements give exactly the same trends.

The lamella area estimate is affected by the lamella thickness value, and hence strongly influenced by the SCB content of the resin. In Figure 10, lamella thickness and lamella area are plotted together as a function of changes in SCB/1000 carbon atoms for PE1-3. PE1-3 are used to illustrate this point because they have similar MW, consequently the effect of SCB can be seen with minimum influence from MW differences. Among the three resins, as the SCB content of the resins increases (Figure 10), lamella thickness values decrease while lamella area values increase.

In earlier sections, plots between crystallinity, lamella thickness and ESCR did not show any meaningful correlations. Resins, such as PE1 and PE7 that have similar SAXS-lamella thickness values, have significantly different ESCR values (Tables 1 and 2). In Figure 11, ESCR is plotted against the lamella area of resins (based on SAXS-lamella thickness values). The graph shows an increasing ESCR with increasing lamella area values, thus verifying the postulation that larger lamella area means a higher probability for occurrence of inter-lamellar linkages, which eventually improves ESCR. By taking into account both MW and SCB influences on the crystalline phase, lamella area values more accurately reflect changes in phase interconnectivity, thus offering a better correlation to ESCR of the resins than simply crystallinity or lamella thickness values.

4 Conclusions

A large body of research exists on crystalline phase influences on ductile deformation behavior of polyethylene. For brittle fracture behavior, the effect of crystallinity on ESCR of polyethylene has remained unclear. It is generally accepted that an increase in the number of inter-lamellar linkages in the amorphous phase would result in decreases in PE crystallinity. Therefore, PE with high ESCR should have low crystallinity. In this study, behavior of resins with similar MW (PE1-3) confirmed this observation. However, correlations between crystallinity and ESCR over resins of different MW showed no meaningful results. Resins with very different ESCR values, such as PE4 and PE8, can have similar crystallinity values. Based on the resins in this study, we conclude that when MW differences are large, overall crystallinity cannot be correlated to ESCR of PE. Attempts to correlate lamella thickness to ESCR showed a similarly ambiguous relationship as that between crystallinity and ESCR.

Inter-lamellar links, which are critical to ESCR of PE, must “anchor” in lamellae as the term suggests. Theorization on the ESCR behavior from the point of interconnectivity between crystalline and amorphous phases leads to the study of the relationship between lamella lateral surface area and ESCR. Unlike crystallinity and lamella thickness that predominantly show SCB effects, lamella area calculations take into account both SCB and MW influences. Our work showed that increasing ESCR is associated with an increasing lamella lateral surface area of PE. Larger lamella lateral surface area increases the probability of inter-lamellar linkage formations, which leads to improved phase interconnectivity and hence, higher ESCR for polyethylene.

Acknowledgements

The authors would like to thank the Natural Sciences and Engineering Research Council (NSERC) of Canada, and the Canada Research Chair (CRC) program of NSERC, for financial support. Many thanks go to Dr. Ariel Gomez and Professor Stefan Kycia, Department of Physics, University of Guelph, Guelph, Ontario, Canada, for their assistance with the X-ray scattering experiments. In addition, the authors are grateful to Exxon Mobil Chemical Canada (Imperial Oil Canada), Nova Chemicals (Canada) Ltd., and Repsol YPF, Spain, for supplying resins.

References

1. Brostow, W. and Corneliussen, R.D. *Failure of Plastics*, Hanser Publishers: New York, 1986.
2. Ward, I. M. *Mechanical Properties of Solid Polymers*, Wiley-Interscience: Toronto, 1971.
3. Keith, H.D. and Padden, F.J. (1959) *J. Polym. Sci.*, 39(135), 123–138.
4. Keller, A. (1959) *J. Polym. Sci.*, 39, 151–173.
5. Till, P.H. (1957) *J. Polym. Sci.*, 24(106), 301–306.
6. Lin, L. and Argon, A.S. (1994) *J. Mat. Sci.*, 29, 294–323.
7. Lu, X., Qian, R., Mcghie, A.R., and Brown, N. (1992) *J. Polym. Sci., Part B: Polymer Physics*, 30(8), 899–906.
8. Stadler, F.J., Kaschta, J., and Muenstedt, H. (2005) *Polymer*, 46(23), 10311–10320.
9. Lu, X., Qian, R., and Brown, N. (1995) *Polymer*, 36(22), 4239–4244.
10. Capaccio, G. and Ward, I.M., (1981) *J. Polym. Sci., Part B: Polymer Physics*, 19, 667–675.
11. Hosoda, S., Nomura, H., Gotoh, Y., and Kihara, H. (1990) *Polymer*, 31, 1999–2005.
12. Bodor, G., Dalcolmo, H.J., and Schroeter, O. (2008) *Colloid and Polymer Science*, 267(6), 480–493.
13. Lustiger, A. and Markham, R.L. (1983) *Polymer*, 24, 1647–1654.
14. Ferry, J. D., *Viscoelastic Properties of Polymers*, 3rd ed., Wiley: New York, 1980.
15. Huang, Y. and Brown, N. (1988) *J. Mat. Sci.*, 23, 3648–3655.
16. Yeh, J. T. and Runt, J. (1991) *J. Polym. Sci., Part B: Polymer Physics*, 29, 371–388.
17. Brown, N., Lu, X., Huang, Y., Harrison, I. P., and Ishikawa, N. (1992) *Plastics Rubber and Composites Processing and Applications*, 17(4), 255–258.
18. Janimak, J. J. and Stevens, G. C. (2001) *J. Mat. Sci.*, 36(8), 1879–1884.
19. Yeh, J. T., Chen, J.-H., and Hong, H.-S. (1994) *J. Appl. Polym. Sci.*, 54(13), 2171–2186.
20. Hittmair, P. and Ullman, R. (1962) *J. Appl. Polym. Sci.*, 6(19), 1–14.
21. Huang, Y.-L. and Brown, N. (1991) *J. Polym. Sci., Part B: Polymer Physics*, 29, 129–137.
22. Munaro, M. and Akcelrud, L. (2008) *Polym. Degrad. Stabil.*, 93, 43–49.
23. Yeh, J.T. and Hong, H.S. (1994) *J. Polym. Res.*, 1(4), 375–383.
24. Van Krevelen, D.W. *Properties of Polymers*, 3rd ed., Elsevier Scientific Publishing Company: New York, 1990.
25. Wlochowicz, A. and Eder, M. (1984) *Polymer*, 25(9), 1268–1270.
26. Kakudo, M. and Kasai, N. *X-Ray Diffraction by Polymers*, Kodansha LTD. and Elsevier Publishing Company: Tokyo, Amsterdam, New York, 1972.
27. Cheng, J.J., Polak, M.A., and Penlidis, A. (2008) *J. Macromol. Sci.: Pure and Applied Chemistry*, 45(8), 599–611.
28. Scheirs, J., Böhm, L. L., Boot, J. C., and Leever, P. S., (1996) *Trends in Polymer Science*, 4(12), 408–415.
29. Simanke, A. G., Galland, G. B., Neto, R. B., Quijada, R., and Mauler, R. S., (1999) *J. Appl. Polym. Sci.*, 74(5), 1194–1200.
30. Manzur, A., (2008) *J. Appl. Polym. Sci.*, 108(3), 1574–1581.
31. Seguela, R., (2005) *J. Polym. Sci. Part B: Polym Phys*, 43(14), 1729–1748.
32. Men, Y.F., Rieger, J., Enderle, H.-F., and Lilge, D., (2004) *European Physical Journal E: Soft Matter*, 15(4), 421–425.
33. Rao, Y., Greener, J., Avila-Orta, C.A., Hsiao, B.S., and Blanton, T.N. (2008) *Polymer*, 49, 2507–2514.
34. Keller, A., (1969) *Colloid and Polymer Science*, 231(1–2), 386–421.
35. Hoffman, J.D., Davis, G.T., and Lauritzen, J.I., Hannay, N.B. *Treatise on Solid State Chemistry*, Plenum: New York, 1976.
36. Bassett, D.C. (2007) *Polymer*, 48, 3384–3387.
37. Alvarado-Contreras, J.A. 2007, *Micromechanical Modelling of Polyethylene*, PhD thesis, Department of Civil Engineering, University of Waterloo, Waterloo, Ontario, Canada.